

## Short communication

## Characterization and thermal performance assessment of earthen adobes and walls additive with different date palm fibers



Abdellah Mellaikhafi<sup>a,\*</sup>, Mohamed Ouakarrouch<sup>c</sup>, Abderrahim Benallel<sup>a</sup>, Amine Tilioua<sup>a,\*</sup>, Mahmoud Ettakni<sup>b</sup>, Abdelhak Babaoui<sup>a</sup>, Mohammed Garoum<sup>c</sup>, Moulay Ahmed Alaoui Hamdi<sup>b</sup>

<sup>a</sup> Research Team in Thermal and Applied Thermodynamics (2.T.A.), Mechanics, Energy Efficiency and Renewable Energies Laboratory (L.M.3.E.R.), Department of Physics, Faculty of Sciences and Techniques Errachidia, Moulay Ismail University of Meknès, B.P. 509, Boutalamine, Errachidia, Morocco

<sup>b</sup> Faculty of Sciences, Department of Physics, Moulay Ismail University of Meknès, Meknès, B.P. 11201 Zitoune, 5000 Meknès, Morocco

<sup>c</sup> Materials, Energy and Acoustics TEAM, Higher School of Technology in Salé, Mohammed V University in Rabat, Morocco

## ARTICLE INFO

**Keywords:**

Thermal insulation  
Date palm fibers  
Adobe  
Thermal properties  
Wall heat flux  
Time lag  
Decrement factor

## ABSTRACT

This study deals on the one hand, with experimental characterization of the thermophysical properties of adobes made from raw earth reinforced with five different plant waste fibers from palm trees in the Drâa-Taïlalet region in southeastern Morocco (Pinnate leaves, Palm fiber mesh, Palm trunk, Petiole and Palm cluster) and on the other hand, with numerical simulation based on the one-dimensional numerical model to evaluate the effect of the wall constructed in studied adobe on the heat flux and the thermal comfort of the building. The results of the experimental study show that the thermal properties of the samples improve and are different depending on the type of fibers incorporated. Indeed, the thermal insulation property improves at least by about 30% for a mass fraction of 6% of the petiole and palm fiber mesh and at most 48% for 6% of the pinnate leaf fibers. Moreover, the adobes containing the Pinnate leaf fibers offer the best insulation property compared to those containing the other four fibers with thermal conductivities of about 0.312 W/(m.K) and 0.265 W/(m.K) respectively for the two mass fractions of 3% and 6%, as well as its rate thermal damping of diffusion is maximum due to its low value of thermal diffusivity. Numerical simulation results show a maximum decrease of about 46% of the flux through the walls contained the fibers of pinnate leaves. In addition, the heat flux time lag and the heat flux decrement factor improve, ensuring good energy efficiency.

## 1. Introduction

In Morocco as in the whole world, the stakes of reducing energy consumption and CO<sub>2</sub> emissions encourage the construction sector in general and that of materials in particular to turn to local and bio-based materials. Raw earth materials can reduce the environmental impact of buildings [1–4] while improving their energy efficiency and thermal comfort [5–10]. Nevertheless, the scientific characterization of raw earth materials and the evaluation of the thermal impact of the addition of fibers to earth materials, are more necessary for a better recognition by all the actors of the construction. In this context, several authors have worked on the thermal and

\* Corresponding authors.

E-mail addresses: [abd.mellaikhafi@gmail.com](mailto:abd.mellaikhafi@gmail.com) (A. Mellaikhafi), [a.tilioua@fste.umi.ac.ma](mailto:a.tilioua@fste.umi.ac.ma) (A. Tilioua).

mechanical characterization of raw earth construction materials. F. Hadji et al. [11] aimed to determine the thermal conductivity, by the hot wire method, of traditional construction materials obtained by mixing two types of earth used in Algeria with different quantities of straw. They showed that the thermal conductivity of all tested samples, with and without straw, is between  $0.1 \text{ W}/(\text{m}^2\cdot\text{K})$  and  $2 \text{ W}/(\text{m}^2\cdot\text{K})$ . To evaluate of the thermal impact of adding sawdust with different percentages to clay materials on earthen building envelopes was performed by M. Charai et al. [12]. In determining the thermal diffusivity, volumetric specific heat and thermal conductivity of sawdust-earth samples using the hot disc method, they showed that the thermal conductivity decreases of 30% and the thermal resistance of earthen building envelopes improves of 31%, for an addition of 10% sawdust. K. Rashid et al. [13] observed in their work, a reduction in bulk density and thermal conductivity up to 18% with an increase in water absorption for earth bricks containing bamboo, jute, coir, sisal and polyester fibers, the thermal conductivity was estimated using finite element simulation on ANSYS platform and the other parameters are measured experimentally. S. Ajouguim et al. [14] sought to improve the mechanical properties and thermal insulation of compacted earth bricks using natural, alkali-treated fibers extracted from the Alfa plant harvested in Northern Morocco (Oujda region). The measurement of thermal conductivity was carried out on the HOT DISK TPS type 150 apparatus, using cylindrical samples ( $1.3 \text{ cm} \times 1.3 \text{ cm}$ ). The results show that compacted earth bricks with 1 wt% of alkali treated esparto fibers have better mechanical properties with low thermal conductivity. In this context, a study of improvement of the mechanical and thermal properties of earthen bricks has been carried out by E. Olacia et al. [15], but this time by adding seagrass fibers. From the results of mechanical tests and measurements of thermal conductivity, they showed an improvement of about 30% that is achieved when this marine plant in this natural arrangement is included at a content of 1.50% or 3% but the thermal conductivity is high compared to that of straw reinforced samples. In addition, P. Muñoz et al. [16] has shown the feasibility of an earthen adobe reinforced with residues from the paper and pulp industry (PPR). They concluded that the thermal conductivity is reduced of about 30% for an addition of 12.5% of PPR while the compressive strength can improve up to 190%. There are also studies that have aimed at improving the hygrothermal performance of construction materials. In this axis, a building plaster has been realized by S. Liuzzi et al. [17] using olive fibers incorporated in the clay matrix. Using experimental hygrothermal measurements validated by a simulation performed by the WUFI Plus software on a test building, analyzing the results in a typical Mediterranean climate, the authors showed a significant energy saving achieved in terms of humidification and dehumidification using this material of biological origin. In this sense, A. Laborel-Préneron et al. [18] have shown that the addition of 6% by weight of straw slightly limits the transport of moisture and reduces of 75% the thermal conductivity of the bricks compared to the earth without any vegetable aggregate. On the other hand, in the oases in southeastern Morocco known by its semi-arid climate, hot in summer and cold in winter, the economy is based primarily on the exploitation of the date palm, which leads to the availability of large quantities of plant waste from renewable parts of date palms without exploitation. According to data from the Regional Directorate of Agriculture of Drâa-Tafilalet, the overall number of palm trees across the region is 4.889 million (May 2019), while the planted area is 47,293 Ha [19]. This leads to an average production of 85,000 tons of dates per year, which produce some 75,000 tons of palm waste each year [20]. In addition, these oases are also known by the presence of various constructions based on raw earth of great value in terms of thermal comfort ensuring coolness in summer and a temperate atmosphere in winter and in terms of historical and architectural culture that characterizes the oasis buildings [21]. From the above, the exploitation of date palm waste fibers for the improvement of thermal properties of building materials and earthen plasters, can be considered as a solution improving the energy efficiency of buildings and as an income-generating activity that can improve the standard of living of oasis farmers by marketing of this product. In this context, a thermomechanical study of raw earth bricks, stabilized with lime and reinforced with aggregates of a mixture of waste components of date palm was conducted by D. Khoudja et al. [22] in Biskra, Algeria, their study, shows an improvement in thermal insulation, with a thermal conductivity of  $0.342 \text{ W}/(\text{m}\cdot\text{K})$  for bricks containing 10% of aggregates while maintaining a minimum performance required by the standards of earth construction. However, the present paper deals with the influence of the nature of plant rejects from the renewable parts of date palms in the oases of the Drâa-Tafilalet region in southeastern Morocco, and their content on the thermal properties of the soil adobes. Five plant fibers, Pinnate leaves, Palm fiber mesh, Palm trunk, Petiole and Palm cluster were added to five soil matrices to obtain weight percentages from 0% to 6%. An experimental study was conducted to present the effects of the addition of each fiber and its content on the following thermal properties: thermal conductivity, thermal diffusivity, volumetric heat capacity and thermal effusivity. Based on these results, a numerical simulation adopted to solve the heat equation with boundary and initial conditions was carried out to evaluate the effects of the addition of date palm fibers on the thermal performance of the earthen walls from the study of the variation of heat flux passing through each wall as well as the time lag of heat flux and the decrement factor. This numerical study was based on the work done by H. Asan et al. [23], X. Jin et al. [24] and C.R. Ruivo et al. [25].

This study therefore aims to compare the thermal properties of adobes containing different fibers of date palm wastes in the oasis of Drâa Tafilalet. The aims is to select and enhance the most energy efficient fibers that could be used by the inhabitants of the oasis as building materials to reduce energy consumption that has been increased in recent years because of the use of cement-based building materials.

## 2. Materials and procedures

### 2.1. Raw materials and manufacture of the samples

The raw soil used in this study was extracted from an area located in the oasis of Tafilalet in southeastern Morocco. This soil was chosen for the study because of its abundance and its traditional use for the manufacture of adobes and rammed earth of good quality by the local population. The five different date palm fibers used: pinnate leaves, Palm fiber mesh, trunk, petiole and cluster, are released from the cuttings of the rejects of palm trees of Tafilalet oasis on the edge of the Wadi Ziz valley in southeastern Morocco (see

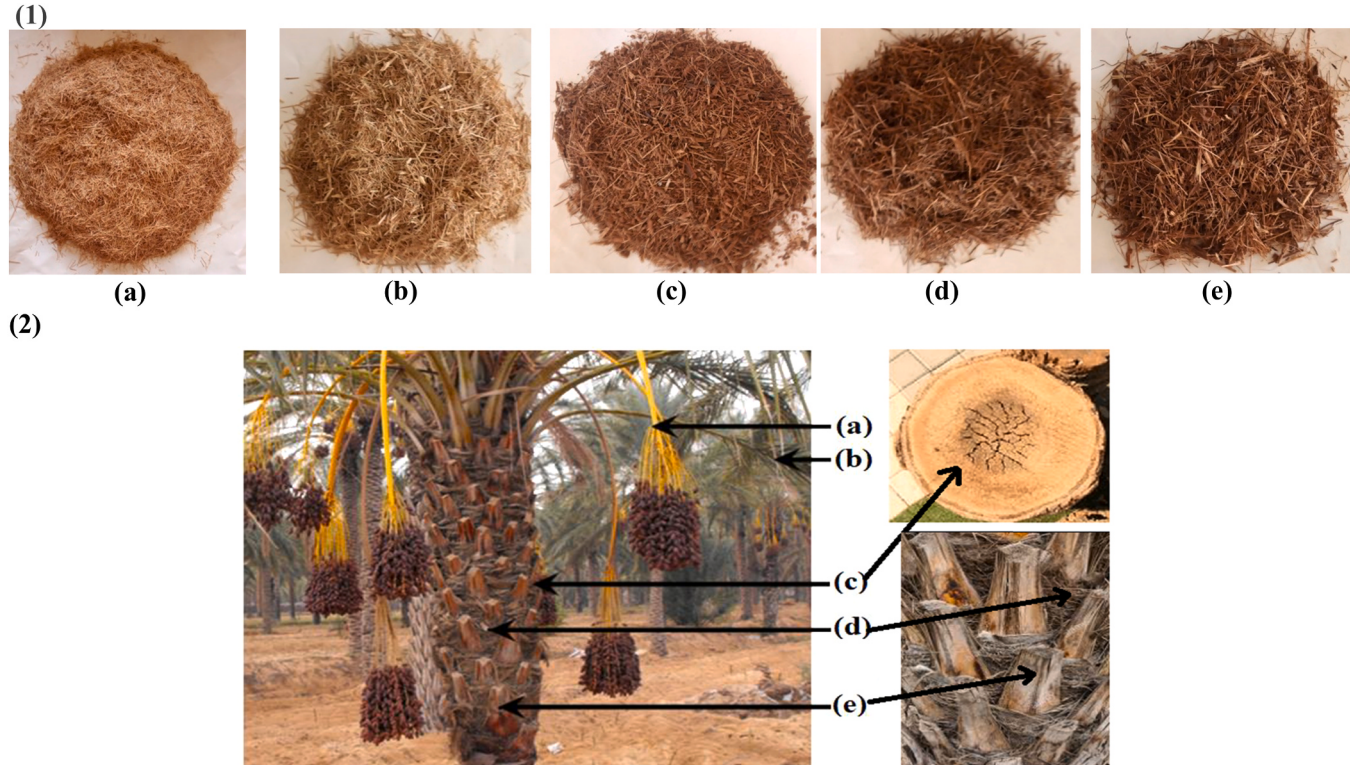


**Fig. 1.** The five date palm fibers (1) and parts (2) used: (a) cluster, (b) pinnate leaves, (c) trunk, (d) palm fibers mesh and (e) petiole.



**Fig. 2.** Picture of soil samples containing palm fibers studied.

**Fig. 1).** Prior to its use, the fibers were washed with water in order to remove polluting particles. Then, these fibers were dried in the sun for five days, then in an oven at 70 °C until dry. The fibers were cut using a grinding machine and were sieved to remove the grains, then the fibers whose length ranged from about 5–10 mm were selected.

Due to low fiber density, we limited the mass fraction to 6% to avoid affecting the mechanical strength of the composite materials. Thus, the weight ratios of 0%, 3%, and 6% of fibers to the dry weight of the soil were tested. From the SEM shown in Fig. 9, we found that the diameters or widths of the fibers are not uniform, and then we measured the volume and mass of compacted fibers to determine its densities using a graduated cylinder and a balance. The range of diameter, volume and density of the fibers used are showed in Table 4.

For sample preparation, the soil was sieved to obtain particle sizes <2 mm and then manually mixed with the fibers without preferential orientation to obtain a homogeneous mixture between the fibers and the soil. We have manually mixed the soil containing the fibers for twenty minutes with 31% water to the dry weight of the soil to obtain a homogeneous mixture with appropriate plasticity for molding the samples.

The amount of water was determined using relationship Eq. (1):

$$W(\%) = (W_L + W_P)/2 \quad (1)$$

Where  $W_L$  is the liquid limit and  $W_P$  is the plastic limit. This value has been used in previous works [26,27]. Cylindrical molds of 110 mm diameter and 22.5 mm thickness were made. These molds were filled with the obtained mixture and the same manual compaction was applied on three layers. The samples were then left to dry in the open air and in the shade for 30 days before being tested in order to avoid thermal shocks which could cause cracks in the clayey matrix (Fig. 2). For comparison purposes, we prepared and characterized a fiber-free sample.

## 2.2. Experimental procedures used

### 2.2.1. Physical, chemical and mineralogical characterization of raw materials

The particle-size analyses of used soil were carried out, according to two techniques, the particle-size analysis by wet sieving of the elements of dimensions higher than 80 µm according to the French standard NF P94-056 [28] and the particle-size analysis by sedimentation of the particles passing through the sieve of 80 µm of opening by using the difference of fall of the particles, in a test tube of 2 l of distilled water according to the French standard NF P94-057 [29]. This last analysis completes the particle size analysis by sieving of a soil. The geotechnical soil characteristics were determined by measuring the Atterberg limits and the water content of the soil leading to the maximum drying density for a compaction energy of 2.7 MJ/m<sup>3</sup> obtained by a modified Proctor test.

X-ray diffraction (XRD), were implemented to evaluate the mineralogical composition of the soil. Measurements were made according the powder method using the PANalytical X'pert Pro MRD diffractometer and the results of the analyses are provided by X'Pert HighScore software. This instrument is equipped with a copper anticathode and uses the copper K $\alpha$  line with wavelength  $\lambda = 1.540456$  Å. This identification of clay minerals from raw soil powder samples (<80 µm) was performed at CNRST (National Center for Scientific and Technical Research) in Morocco. Morphological analysis of soil and date palm fibers and semi-quantitative analysis of chemical elements were performed using a Quanta 200 scanning electron microscope (SEM) coupled to an energy dispersive X-ray spectrometer (EDX) in the CNRST scanning electron microscopy laboratory. The SEM instrument operates at 30 KV while the EDX is attached to the SEM, and has a microanalysis resolution of 133 eV.

### 2.2.2. Thermo-physical characterization method

#### 2.2.2.1. Thermal conductivity measurement.

The thermal conductivity of all samples was measured using the hot plate method in steady-state regime. The principle of this method is illustrated in Fig. 3. Its experimental device consists of a heating element inserted

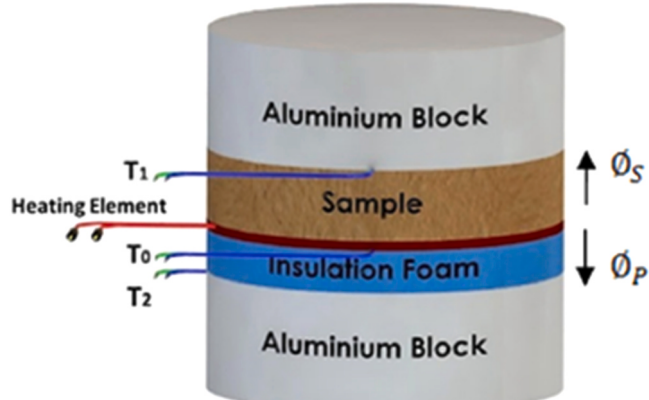


Fig. 3. Schema of hot plate method in a steady-state regime.

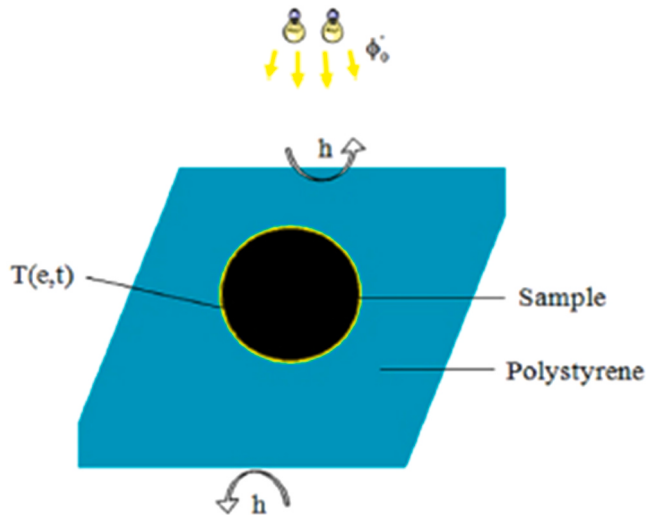


Fig. 4. Schema of flash method.

between the characterized sample and an insulating polyethylene foam, having an electrical resistance  $R_e = 38 \Omega$  and a size  $(150 \times 150 \times 0.2) \text{ mm}^3$ . The assembly is placed between two aluminum blocks to have a constant temperature on the unheated faces. The heating element emits a uniform thermal flux through the front faces of the sample and the insulating foam. K-type thermocouples positioned in the center of the faces record the temperature evolution of the faces. The heat flows transmitted through the polyethylene foam  $\phi_p$  and the sample  $\phi_s$  are assumed to be unidimensional. The thermal conductivity of the sample is calculated when the steady state is established, using Eq. 2 and Eq. 3.

$$\phi_T = \frac{U^2}{R_e S} = \phi_s + \phi_p \quad (2)$$

$$\lambda_s = \frac{e_s}{T_0 - T_1} \times \left[ \frac{U^2}{R_e S} - \frac{\lambda_p}{e_p} (T_0 - T_2) \right] \quad (3)$$

Where  $\lambda_p$  and  $\lambda_s$  are the thermal conductivity of the polyethylene foam and the characterized sample, respectively.  $U$ ,  $R_e = 40\Omega$  and  $S$  are the heating element voltage, the electrical resistance and the heating element surface, respectively.  $e_p$  and  $e_s$  represent the thickness of the polyethylene foam and the characterized sample, respectively.  $T_0$  is the temperature at the center of the bottom surface of the heating element,  $T_1$  is the temperature measured on the unheated face of the sample, and  $T_2$  is the temperature of the unheated face of the polyethylene.

**2.2.2.2. Thermal diffusivity measurement.** The thermal diffusivity of the samples has been estimated using the flash method in a transient thermal regime. Its principle is described in Fig. 4. A high-power light flux is sent on one of the faces of a parallel sample for a

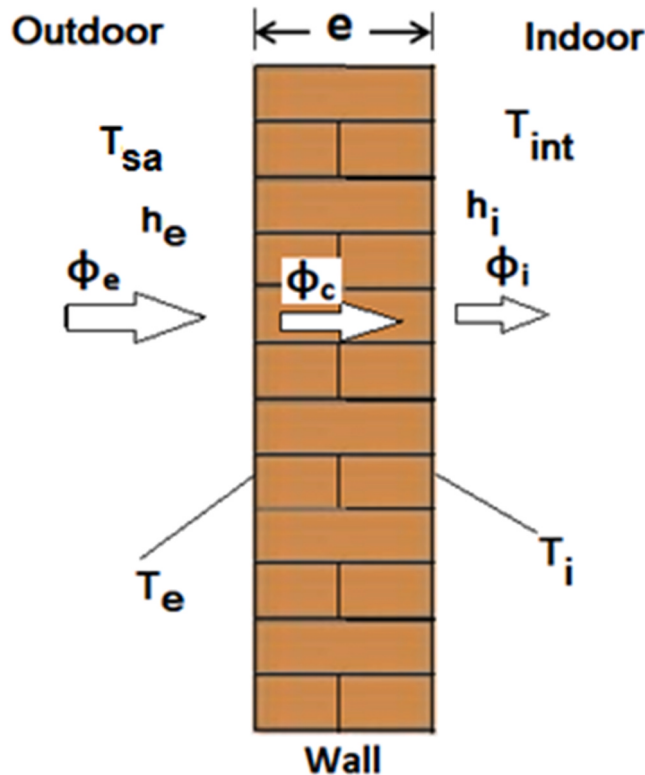


Fig. 5. The heat transfer in the studied walls.

very short time ( $t_d = 8$  s). The sample has been tinted in black in order to absorb the totality of the light flux received by its surface. Then, it is surrounded by a polystyrene ring to minimize the thermal losses on the sides (Fig. 4). A thermocouple in contact with the back face allows recording the rise of its temperature from the moment when the front face received the flash. A model of heat transfer in the sample has allowed several authors to propose methods for estimating the thermal diffusivity from the experimental thermograms. In this work, the method developed is based on global minimization. Considering that the absorbed light flux is uniform over the entire front face of the sample, the lateral heat losses are negligible, the heat transfer is one-dimensional and the initial temperature  $T_0$ , at  $t = 0$ , is equal to the ambient temperature. We can then write:

$$\frac{\partial^2 T(x, t)}{\partial x^2} = \frac{1}{a} \frac{\partial T}{\partial t} \quad (4)$$

$$\text{Où: } \left\{ \begin{array}{l} \left( \frac{\partial T(x, t)}{\partial x} \right)_{x=0} = -h_1 \cdot T(0, t) + \phi_0 \cdot g(t) \\ \left( \frac{\partial T(x, t)}{\partial x} \right)_{x=e} = -h_2 \cdot T(e, t) \\ g(t) = \begin{cases} \frac{1}{t_d} & \text{if } 0 < t < t_d \\ 0 & \text{if } t_d < t \end{cases} \\ T(x, 0) = 0 \end{array} \right\}$$

Where:  $a$  denotes the thermal diffusivity,  $h_1$  and  $h_2$  are the overall heat transfer coefficients of the two faces of the sample under study,  $\phi_0$  presents the thermal energy absorbed at the boundary face ( $x = 0$ ),  $g(t)$  is the time dependence of the thermal energy generation.  $\phi_0 \cdot g(t)$  refers to the finished pulse of a flash duration  $t_d$ .

The transformation of Eq. 4 in Laplace space will give the following equation:

$$\theta(e, p) = \frac{j \cdot T_{max} \cdot F(p)}{\left[ \operatorname{Cosh}(\sqrt{jp}) \cdot (b_{11} + b_{12}) + \operatorname{Sinh}(\sqrt{jp}) \left[ \frac{jp + (b_{11} \cdot b_{12})}{\sqrt{jp}} \right] \right]} \quad (5)$$

$$\text{With: } j = \frac{e^2}{a}$$

$F(p)$  indicate the Laplace transform of  $g(t)$ ,  $b_{i1}$  and  $b_{i2}$  present the Biot numbers,  $T_{\max}$  is the adiabatic limit temperature and  $e$  is the sample thickness.

$$F(p) = \frac{1 - e^{-p \cdot t_d}}{p \cdot t_d}; b_{i1} = \frac{h_1 e}{\lambda}; b_{i2} = \frac{h_2 e}{\lambda} \text{ and } T_{\max} = \frac{\phi_0}{\rho c e}$$

The expression of the theoretical temperature  $T_h$  of the backside of the sample was obtained by the numerical inversion of Eq. 5 as a function of the parameters  $a$ ,  $e$ ,  $b_{i1}$ ,  $b_{i2}$ ,  $T_{\max}$  and  $t$  which will be estimated from the experimental data. Their optimal values can be obtained by minimizing the squared distance between the thermogram and the theoretical experimental thermogram (Eq. 6) as described in [30]. A computational code has been implemented in the Mathematica language that allows us to solve the minimization equation.

$$M(e, T_{\max}, a, b_{i1}, b_{i2}) = \sum_{(i=1)}^N [T_{\exp}(t_i) - T_h(e, T_{\max}, a, b_{i1}, b_{i2}, t_i)]^2 \quad (6)$$

### 2.3. Mathematical and numerical model

The heat transfer in the wall shown in Fig. 5 is assumed to be one-dimensional. The exterior and interior wall surfaces are subject to convective heat flow with the exterior and interior air respectively.

The heat transfer equation in the wall is expressed by Eq. 4.

The boundary conditions at the inner and outer wall surface are as follows:

$$-\lambda \frac{\partial T}{\partial x} = h_{\text{ext}} (T_{\text{sa}} - T_e) \quad \text{For } x = 0 \quad (7)$$

$$-\lambda \frac{\partial T}{\partial x} = h_{\text{int}} (T_i - T_{\text{int}}) \quad \text{For } x = e \quad (8)$$

Where  $h_{\text{ext}}$  and  $h_{\text{int}}$  are the two convective heat transfer coefficients at the exterior surface and interior surface respectively and  $\lambda$  is the thermal diffusivity.  $T_e$ ,  $T_i$  and  $T_{\text{int}}$  are the temperatures of the exterior wall surface, interior wall surface and indoor air respectively. In addition, the outdoor temperature  $T_{\text{sa}}$  was considered as the solar-air temperature, which is assumed to have sinusoidal variations during a 24-hour period [23].  $T_{\text{sa}}$  is calculated by the relation (Eq. 9):

$$T_{\text{as}}(t) = \frac{T_{\max} - T_{\min}}{2} \sin\left(\frac{2\pi t}{P} - \frac{\pi}{2}\right) + \frac{T_{\max} - T_{\min}}{2} + T_{\min} \quad (9)$$

Where,  $T_{\max}$  and  $T_{\min}$  are the maximum and minimum outdoor temperatures, respectively and  $P$  the period.

In this study, we considered the model cited in [24],  $T_{\max} = 35^\circ\text{C}$ ,  $T_{\min} = 25^\circ\text{C}$ ,  $T_{\text{int}} = 26^\circ\text{C}$ ,  $h_{\text{ext}} = 18.6 \text{ W}/(\text{m}^2 \cdot \text{K})$  and  $h_{\text{int}} = 8.7 \text{ W}/(\text{m}^2 \cdot \text{K})$ . The initial condition of the temperature in the wall is assumed to be linear at the beginning and it is given as follows

$$T(x, t = 0) = T_{\min} + \frac{(T_{\text{int}} - T_{\min}) \cdot x}{e} \quad (10)$$

The numerical approach adopted to solve Eq. 6 with boundary and initial conditions, is the finite difference method supported by the explicit formulation. To evaluate the effects of the addition of date palm fibers on the thermal performance of the studied walls, we proposed to study the variation of the heat flux passing through each studied wall  $\phi_c$ , the outdoor heat flux  $\phi_e$  and the indoor heat flux  $\phi_i$  as well the heat flux time lag  $\phi$  and the decrement factor  $f_d$ . These last two parameters are calculated by the following Eq.11 and Eq.12.

$$\varphi = \tau_{\phi_{i,max}} - \tau_{\phi_{e,max}} \quad (11)$$

$$f_d = \frac{\phi_{i,max} - \phi_{i,min}}{\phi_{e,max} - \phi_{e,min}} \quad (12)$$

Where  $\tau_{\phi_{i,max}}$  is the time that the interior surface heat flux of the wall is being maximum and  $\tau_{\phi_{e,max}}$  is the time that the exterior surface heat flux of the wall is being maximum.  $\phi_{i,max}$  and  $\phi_{i,min}$  are the maximum and the minimum heat flux of the interior surface of the wall, respectively.  $\phi_{e,max}$  and  $\phi_{e,min}$  are the maximum and the minimum heat flux of the exterior surface of the wall, respectively.

**Table 1**

Comparison of simulation results between the method cited in [24] and the method used in this work.

Method used by	maximum exterior surface heat flux (W/m <sup>2</sup> )	Maximum interior surface heat flux (W/m <sup>2</sup> )	heat flux time lag (h)	Heat flux decrement factor
[24]	37.8	10.8	10	0.1154
<b>Present</b>	37.42	10.77	9.79	0.1185
<b>Relative difference (%)</b>	1	0.28	2.1	2.68

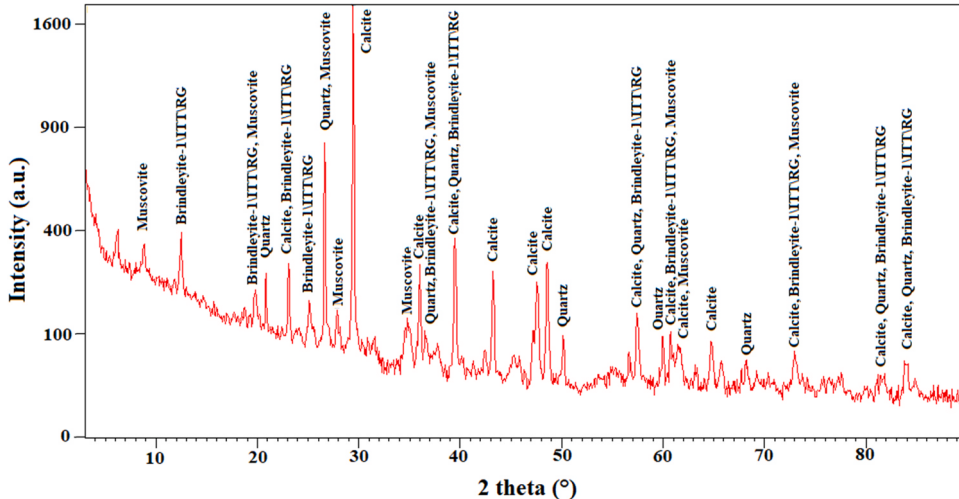


**Fig. 6.** XRD pattern for the soil studied.

Table 2

Identified patterns list of the soil studied.

Compound Name	Chemical Formula	Mineral percentages (%)
Calcite	$\text{CaCO}_3$	32.2
Quartz	$\text{SiO}_2$	26.5
Nimesite-Brindleyite	$(\text{Ni}_2\text{Al}) (\text{AlSi})_5 (\text{OH})_4$	18
Muscovite	$\text{H}_2 \text{K Al}_3 \text{Si}_3 \text{O}_1$	15.44
Zeolite X-FAU	$\text{Na}_{17.52} \text{Al}_{24} \text{Si}_{24} \text{O}_{96} \text{H}_{4.68}$	7.86

Table 3

## Results of particle size distribution analysis, plasticity test and modified Proctor test.

Particle size distribution	Recommended limits of adobe [31]	Atterberg limits (%)		Recommended limits of adobe [31]	Modified Proctor tests	
55% sands	50–70%	PI	16	10–25%	OMC (%)	15.1
25% Silt	15–25%	WP	23	10–25%	$\gamma_{dmax}$ (g/cm <sup>3</sup> )	1.8
17% Clay	10–20%	WL	39	25–45%	$\gamma_s$ (g/cm <sup>3</sup> )	2.60

In order to validate the numerical model, a comparison was made with the numerical results published by X. Jin et al. [24] for a wall of 240 mm thickness with thermal conductivity of 0.62 W/(m.K), and thermal capacity of 1.512 MJ/(m<sup>3</sup>.K). This work showed the variations of temperatures and heat fluxes of the wall every two hours during a day using the discretization of the heat equation by the finite difference method and the implicit scheme is applied in time. The results of the comparison are shown in [Table 3](#). The simulation results obtained from the two methods presented in [Table 1](#) show a maximum relative difference of about 2.7%.

**Table 4**

Chemical composition [33], diameter, density and volume of each type of fiber.

Fibers	Total Extractives (%)	Cellulose (%)	Hemicelluloses (%)	Lignin (%)	Diameter or width ( $\mu\text{m}$ )	Density (kg/m <sup>3</sup> )	Volume (3%) (cm <sup>3</sup> )	Volume (6%) (cm <sup>3</sup> )
Trunk	25.15	39.37	30.31	30.32	536–908	186	51.0	101.9
Pinnate leaves	32.86	47.14	16.13	36.73	780–1210	196	48.4	96.7
Cluster	9.75	43.05	27.48	29.47	290–540	265	35.8	71.5
Palm fibers mesh	7.78	47.50	12.64	39.86	201–856	201	47.1	94.3
Petiole	24.90	43.05	31.34	25.61	94–212	181	52.3	104.7

### 3. Results and discussion

#### 3.1. Mineralogical and geotechnical characterization of the soil

The mineralogical composition of the studied clays was determined by means of X-ray diffraction analyses, the measurements of which are plotted in Fig. 6. The conversion of the peaks into d-spacings of the spectra presented in this figure, allowed us to identify the minerals existing in the studied soil and the results of the analyses are presented in Table 2. The presence of high contents of calcite ( $\text{CaCO}_3$ ) and quartz ( $\text{SiO}_2$ ) minerals estimated at 32.2% and 26.5% respectively is noted. This result is confirmed by the high peaks of calcite and quartz in the spectrum of Fig. 6. Moreover, Nimesite ( $(\text{Ni}_2\text{Al})(\text{AlSi})\text{O}_5(\text{OH})_4$ ), Muscovite ( $\text{H}_2\text{KAl}_3\text{Si}_3\text{O}_{12}$ ) and Zeolite X ( $\text{Na}_{17.52}\text{Al}_{24}\text{Si}_{24}\text{O}_{96}\text{H}_{6.48}$ ) are also significantly present in the studied soil in estimated contents respectively of 18%, 15.44% and 7.86%. On the other hand, the soil EDX presented in Fig. 7.b indicates the presence of chemical element Ti contents probably corresponding to the mineral titanium antigorite presented in rod-shaped form observed on SEM in Fig. 7.a or the mineral titanium dioxide  $\text{TiO}_2$  [21].

The particle size analysis, (see Fig. 8), shows that the studied soil is composed of 4% gravels, 55% sands 25% silt and 17% clay. According to the seismic regulations for earthen constructions in Morocco [31], the manufacture of adobes requires a particle size distribution in the area limited by the contents of clay 10–20%, silt 15–25% and sand 50–70%. This soil is well recommended then for the manufacture of adobes and contains clay content necessary for the cohesion of its elements. The plasticity test indicated that this earth is moderately plastic. Indeed, the plasticity index (PI), the liquid limit ( $W_L$ ) and the plasticity limit ( $W_p$ ) were respectively 16%, 39% and 23%. According to the seismic regulations for earthen constructions in Morocco [31], a good adobe must have Atterberg limits composed of PI and  $W_p$  are between 10% and 25% and  $W_L$  between 25% and 45%. This indicates that the studied earth plasticity was consistent with adobe construction. The results of the modified Proctor tests carried out on the soil allow us to construct the variation of the dry density  $\gamma_d$  as a function of the moisture content  $W(\%)$  by using a series of experimental points. We then obtained a curve whose shape can define a maximum value of dry density noted  $\gamma_{d\max}$  which corresponds to an optimum moisture content noted OMC. We found  $\gamma_{d\max} = 1.8 \text{ (g/cm}^3)$  and OMC = 15.1% and  $\gamma_s = 2.6 \text{ (g/cm}^3)$  which presents the dry density of soil used. Table 3 summarizes the results of the geotechnical tests performed on the soil studied, which are shown above.

#### 3.2. SEM micrographs, EDX analysis spectrum and chemical composition of fibers

The EDX analysis spectrum (Fig. 9) of the fibers from the five dried date palm rejects reveals a very high amount of carbon and oxygen as constituents of these materials. The other minor constituents are clay minerals, potassium oxide, chlorine, and calcium in all fibers and quartz, aluminum, and magnesium in the fibers, petiole, palm, and pinnate leaf fibers. These minerals may be contaminations that were not removed by washing. This result was confirmed by the presence of the shiny particles adhering to the surface of the date palm fibers, indicated by the SEM images Fig. 9. In addition, SEM micrographs of these fibers also show in Fig. 9 veins oriented parallel to the fiber axis and rough fiber surfaces. These structures may favor their mechanical coupling with the clay matrix and this may influence the post-pic behavior of adobes [26]. In addition, the date palm (*Phoenix dactylifera L.*) constitutes, for the Saharan and pre-Saharan regions of Morocco, the essential element of the oasis ecosystem [32]. The chemical compositions of the five date palm fibers are presented in Table 4 [33].

#### 3.3. Thermo-physical characterization

In this section, the effects of different date palm fibers on the thermophysical properties of the composite material in the dry state are presented. Thermal conductivity, thermal diffusivity, apparent density, volumetric heat capacity and thermal effusivity are discussed. The prepared samples (see Fig. 2) were dried in an oven at a constant temperature of  $105 \pm 1 \text{ }^\circ\text{C}$  with an ambient humidity of about 28%. The drying was stopped when the mass of the sample was constant at  $\pm 2 \text{ g}$ .

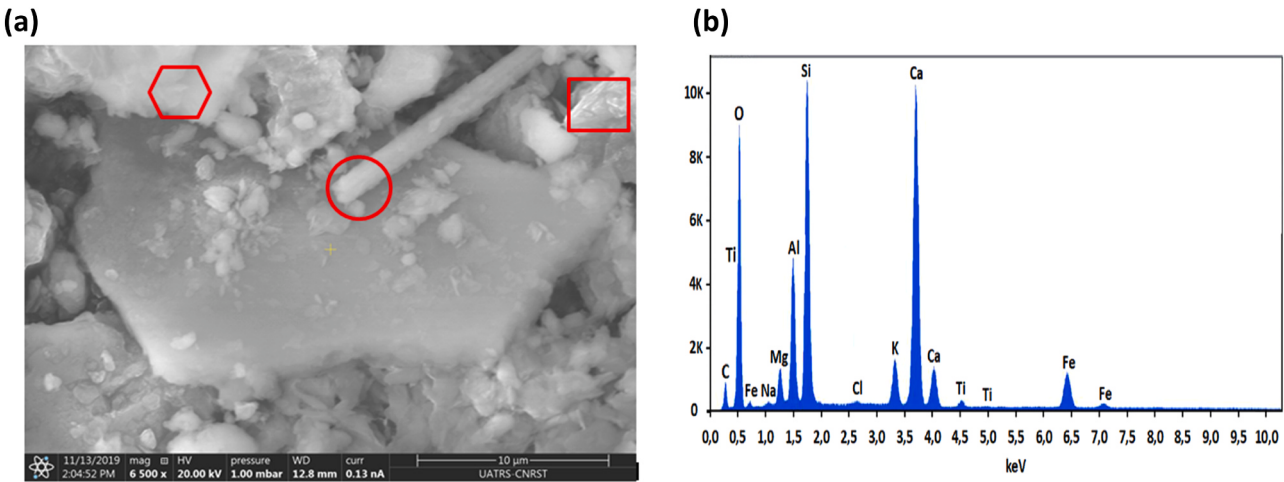


Fig. 7. a) SEM images of studied soil: ○ antigorite rod particle [21], □ quartz and ◻ calcite b) energy-dispersive X-ray spectroscopy (EDX) of studied soil.

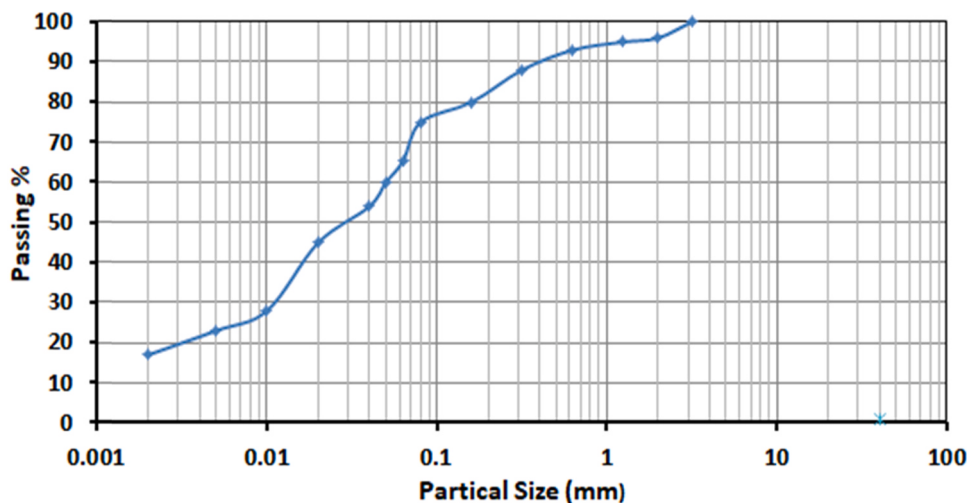


Fig. 8. Particles size distribution of used earth.

### 3.3.1. The apparent density of studied samples

In this study, the apparent density was determined after the drying of the samples by considering the ratio between the mass of the cylindrical block of soil, measured with a balance, and its volume, which is calculated from the measurement of diameter and thickness by means of an electronic caliper with a systematic error of  $\pm 0.01$  mm. Table 5 shows the variation of the apparent density of the manufactured samples as a function of the contents of the five date palm fibers. It was found that the density decreased with the increase of the fibers. The highest decrease was noticed for the sample containing petiole fiber estimated to be about 22% for 3% and 29% for 6% of this fiber. In addition, the other four samples containing Palm fiber mesh, pinnate leaf fibers, trunk fibers and cluster fibers, present almost the same decrease in density estimated on average at about 20% for 3% and 25% for 6% of these fibers.

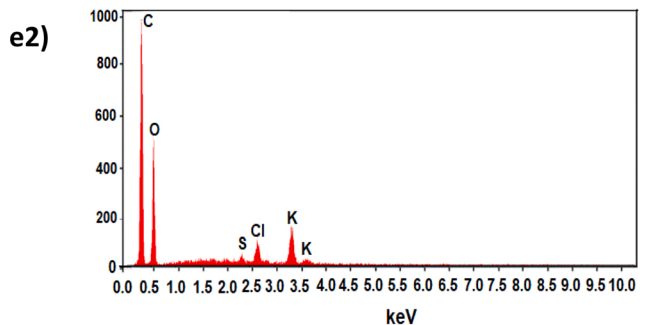
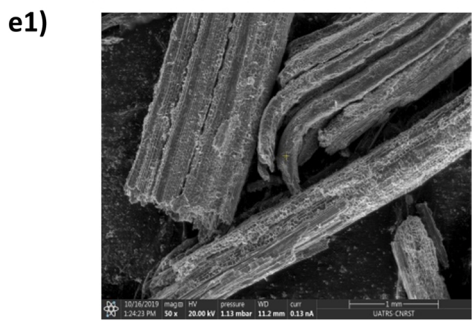
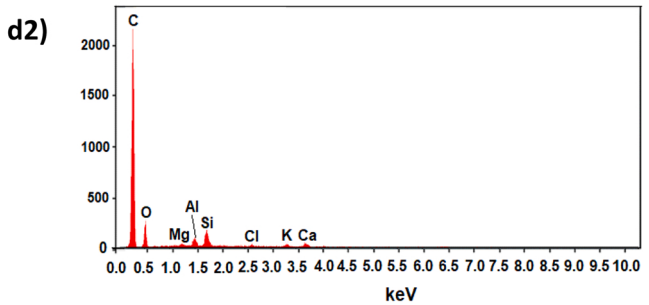
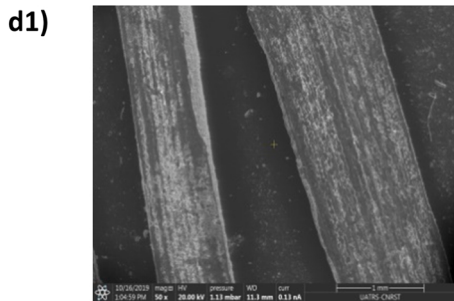
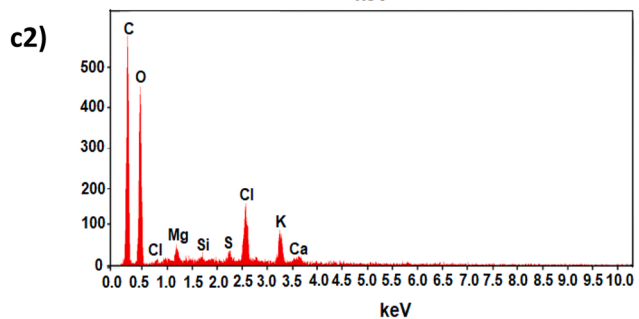
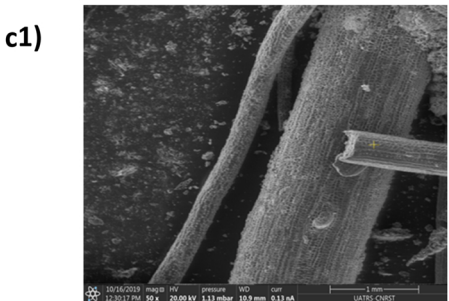
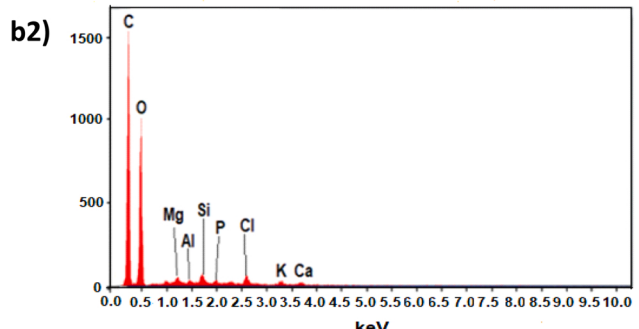
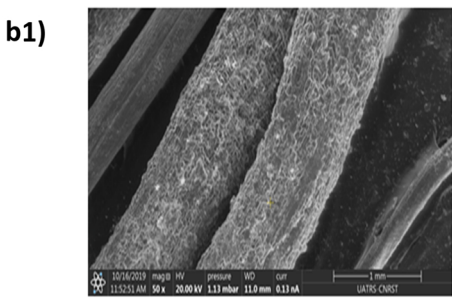
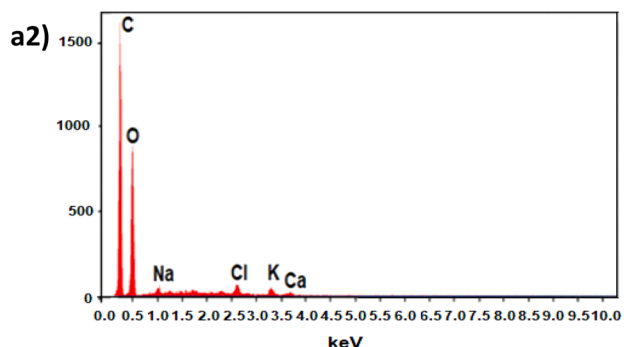
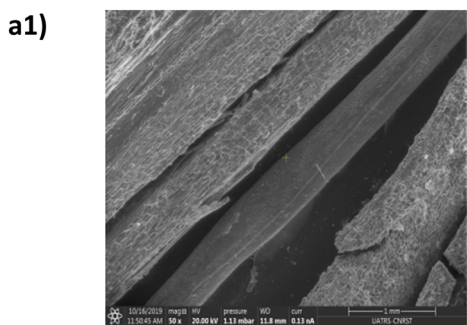
### 3.3.2. Thermal conductivity of studied samples

Thermal conductivity is an important quantity to characterize the capacity of construction materials to conduct heat. Fig. 10.a shows the variation of thermal conductivity as a function of incorporated fiber content for the different biocomposites prepared. We notice firstly, a decrease of the thermal conductivity with the increase of the fiber content and secondly, that the samples containing pinnate leaf fibers present a good insulation property compared to the other samples, because of the decrease of the thermal conductivity from 0.512 W/(m.K) for the sample without fibers to 0.312 W/(m.K) for the sample containing 3% of these fibers and to 0.265 W/(m.K) for the one containing 6%, which leads to an improvement of thermal insulation performance estimated respectively of 39% and 48%. In addition, the thermal conductivities of the other samples prepared with fibers of, trunk, Palm fiber mesh, petiole and cluster are also decreased respectively until 0.304 W/(m.K), 0.355 W/(m.K), 0.354 W/(m.K) and 0.355 W/(m.K), for the case of a fiber content of 6%. These results can be explained, on the one hand, by the progressive increase in the amount of fibers with very low thermal conductivity and by the decrease in the density of the samples (Fig. 10. b) due to the increase in the content of fibers incorporated in the composites that can create pores in the sample that fill with air [23]. On the other hand, by the high contents of cellulose that presents insulating properties characterized by the high permeability of air in the fibers [34] noticed from SEM micrographs of fibers in the form of pores.

This last explanation remains limited and depends on other parameters such as the fragmentation of fibers and the homogeneity of cellulose in the fibers [cellulose2]. Indeed, the fibers of the pinnate leaves have the highest cellulose content which confirms the lowest thermal conductivity of the samples containing these fibers, while the trunk has a lower cellulose content of 39.37% than the other four fibers. However, the sample containing these fibers has a lower thermal conductivity and density than those containing petiole, bunch and palm fiber (see Table 4).

### 3.3.3. Thermal diffusivity and volumetric thermal capacity of studied samples

Fig. 11.a shows the evolution of thermal diffusivity, which characterizes the speed of heat propagation in a material, as a function of the date palm fiber content of the different composite materials studied. This figure shows that the heat diffusion in the sample containing 6% fibers of, pinnate leaves, petiole, cluster, trunk and Palm fiber mesh, is reduced to 26%, 22%, 20%, 15% and 10% respectively. This damping of heat diffusion is due to the alveolar structure of the fibers which is opposed to the heat flow and to the creation of pores within the biocomposites [35]. This characteristic of the fibers in the adobe is important in the thermal insulation to



(caption on next page)

**Fig. 9.** SEM micrographs of fibers of: a1) Palm trunk, b1) Petiole, c1) Palm fiber mesh, d1) Pinnate leave and e1) Palm cluster. EDX analysis spectrum of fibers of: a2) Palm trunk, b2) Petiole, c2) Palm fiber mesh, d2) Pinnate leaves, and e2) Palm cluster.

delay the transmission of heat. The volumetric thermal capacity of a material is its capacity to store heat related to its volume; it characterizes the thermal inertia of construction materials. The volumetric thermal capacity  $\rho.c$  of the studied composite materials was calculated from the results of experimental measurements of thermal conductivity  $\lambda$  and thermal diffusivity  $a$ , with the relation (Eq. 13).

$$\rho.c = \frac{\lambda}{a} \quad (13)$$

**Fig. 11.b** shows the variation of the volumetric thermal capacity of the samples as a function of the fiber contents of the five different palm fibers added. On the one hand, we observe a decrease, in general, of the volumetric thermal capacity with the increase of the content of fibers and on the other hand, the samples containing the fibers of pinnate leaves and the fibers of trunk, present the same decrease of the volumetric thermal capacity  $\rho.c$  until 973 kJ/(m<sup>3</sup>. K) for 3% of these fibers followed by a slight increase estimated of about 1010 kJ/(m<sup>3</sup>. K) for 6% of these fibers. Whereas,  $\rho.c$  increases slightly to 1480 kJ/(m<sup>3</sup>. K) for the sample containing 3% cluster fibers before decreasing to 1263 kJ/(m<sup>3</sup>. K) for 6%. These results are due firstly, to the combined effects of thermal conductivity and thermal diffusivity on the volumetric heat capacity and secondly, to the decrease in density  $\rho$  due to the increase in the formation of pores that fill with air, caused by the increase in fiber contents.

### 3.3.4. Thermal effusivity of studied samples

The thermal effusivity  $b$  of a material characterizes its capacity to exchange thermal energy at its surface with its environment.  $b$  is calculated from the results of conductivity measurements and the calculated values of the volumetric heat capacity, by the relation (Eq. 14).

$$b = \sqrt{\lambda \cdot \rho \cdot c} \quad (14)$$

**Fig. 12** shows the variation of thermal effusivity as a function of fiber content. It can be seen that the thermal effusivity of the five studied samples, decreases with increasing fiber content. This decrease is significant in both cases of the addition of pinnate leaf fibers and the addition of trunk fibers and is estimated at 40% and 36% respectively, for 6% of these fibers. However, the thermal effusivity of the other samples is decreased by about 27%, 22% and 21% for 6% of the palm fiber mesh, cluster and petiole fibers respectively. These results show that the composite material containing pinnate and trunk fibers can retain heat for quite a long time because it slowly dissipates from its surface as soon as the temperature of its environment decreases.

## 4. Numerical simulation results

In this section, we are limited to investigate the effects of thermal properties of pinnate leaf, trunk and cluster fibers on the variation of the heat fluxes of the wall constructed by earthen adobes and on the variations of heat flux time lag and heat flux decrement factor.

### 4.1. Variations and distribution of temperatures and heat flux in the wall constructed by earthen adobes without fibers

**Fig. 13** shows the variations of temperatures  $T_{ext}$ ,  $T_e$ ,  $T_c$ ,  $T_i$  and  $T_{int}$  and heat fluxes  $\varphi_e$ ,  $\varphi_c$  and  $\varphi_i$  of wall constructed by earthen adobes without fibers during four days of simulation.  $T_c$  is the temperature in the center of the wall. The thermal conductivity and volumetric heat capacity of the wall, assumed to be those of the earthen adobe without fibers studied above, are 0.512 W/(m.K) and 1446.33 kJ/(m<sup>3</sup>. K) respectively, and the thickness of the wall is 0.24 m.

**Table 5**

Apparent density as a function of fibers content in samples.

Fibers	Fibers content (%)	Apparent density of the manufactured samples (kg/m <sup>3</sup> )	
	0%	3%	6%
Palm cluster	1586.3	1262.9	1173.2
Palm fiber mesh		1285.6	1167.1
Palm leaf pinnate		1261.2	1197.8
Petiole		1240.5	1122.3
Palm trunk		1249.7	1186.8

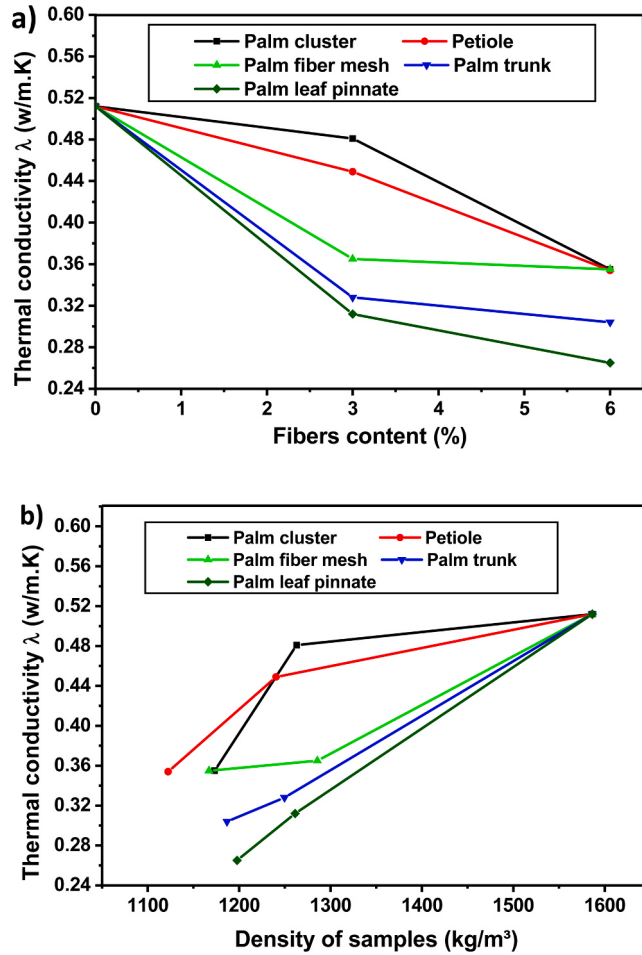


Fig. 10. Thermal conductivity as a function of: a) fibers content in samples and b) density of samples.

As shown in this figure, we have noticed periodic variations of temperatures and fluxes in the wall. These variations have maximum outdoor air, exterior surface, and interior surface temperatures of approximately  $35^\circ\text{C}$ ,  $33.5^\circ\text{C}$ , and  $27^\circ\text{C}$ , respectively, and maximum exterior wall surface and interior wall surface heat fluxes of approximately  $34.6 \text{ W/m}^2$  and  $9 \text{ W/m}^2$ , respectively. The heat flux time lag is about **10.8 h**, and the decrement factor of the heat flux is about **0.14**.

#### 4.2. Effect of thermophysical properties of fibers on heat flux through the wall

The adding of palm fibers to the earthen construction material has influence not only on the temperature distribution in walls and but also on the heat flux passing through these walls. Fig. 14a shows the different variations of heat flux  $\Phi_e$  passing through the walls constructed using different adobes containing the following palm fibers, pinnate leaf fibers, and trunk fibers and cluster fibers. The thickness of the wall is  $0.24 \text{ m}$ . It can be seen that the maximum flux passing through the earth wall without fibers is the highest at about  $14.2 \text{ W/(m}^2\text{. K)}$  and the maximum flux passing through the earth wall containing the fibers of pinnate leaves is the lowest at about  $8 \text{ W/(m}^2\text{. K)}$ . In addition, the maximum flux is about  $10.4 \text{ W/(m}^2\text{. K)}$  in the case of cluster fiber walls and about  $9.2 \text{ W/(m}^2\text{. K)}$  in the case of trunk fiber walls. These results are confirmed by Fig. 14b which shows the hourly average heat flux per day  $\Phi_{cm}$  passing through the studied walls. It indicates that the fluxes  $\Phi_{cm}$  of the walls constructing by earthen adobes without fiber, earthen adobes containing 6% of cluster fibers, earthen adobes with 6% of trunk fibers and earthen adobes with 6% of pinnae leaf fibers are about  $71.1 \text{ W/(m}^2\text{. K)}$ ,  $49.1 \text{ W/(m}^2\text{. K)}$ ,  $45.6 \text{ W/(m}^2\text{. K)}$  and  $38 \text{ W/(m}^2\text{. K)}$ , respectively. Consequently, we have shown a significant reduction in the average flux through the studied walls of about 30.87%, 35.83% and 46.52% respectively in the three cases of adding the fibers indicated above. This result can be explained by the decrease in thermal conductivity which reduces the total heat flux

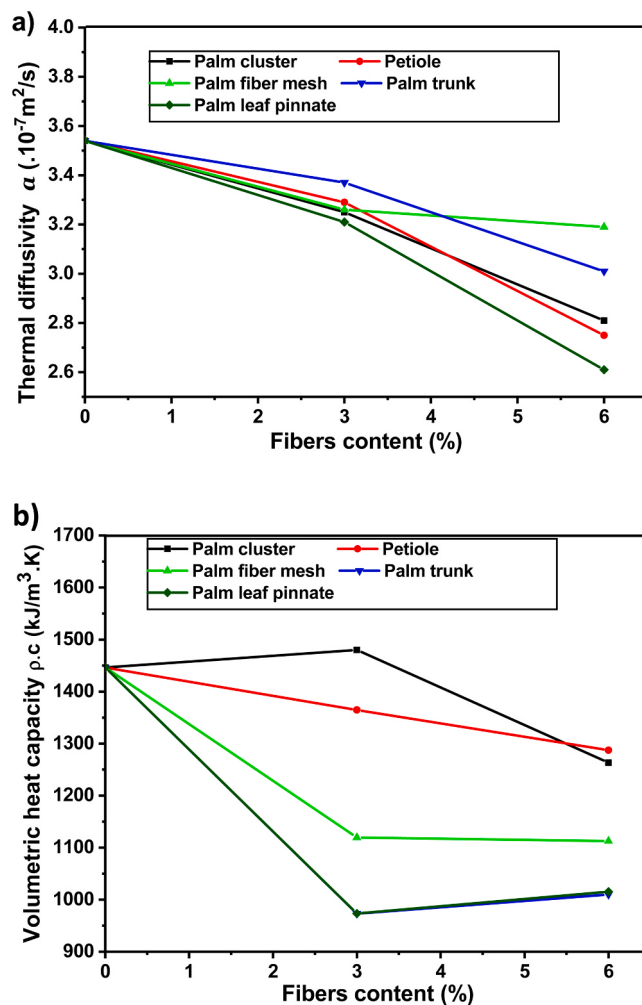


Fig. 11. a) Thermal diffusivity and b) Volumetric heat capacity as a function of percentage of fibers of samples.

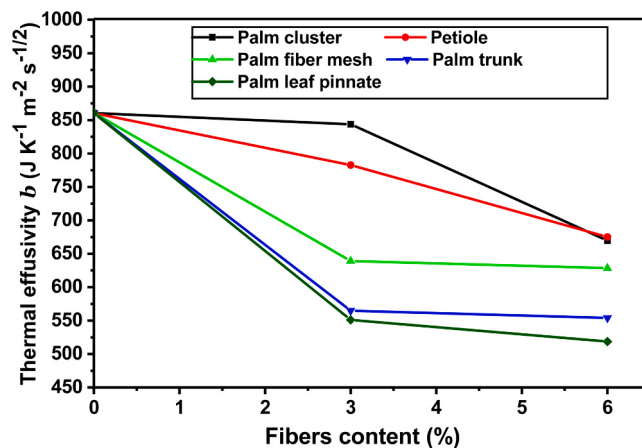
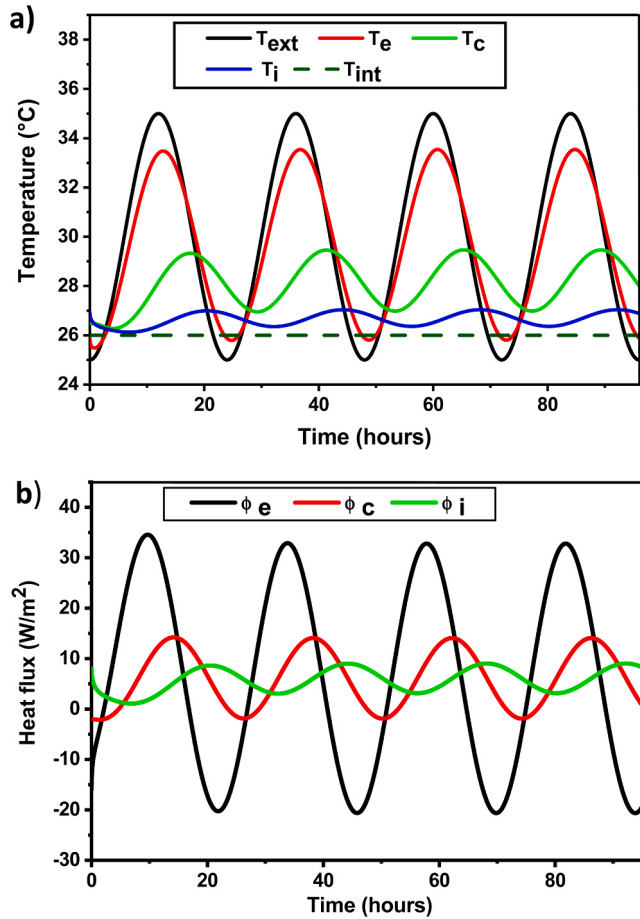


Fig. 12. Thermal effusivity as a function of fibers content of samples.



**Fig. 13.** The variations of temperatures and heat fluxes in the wall built with clay bricks without fibers: a) Temperatures and b) heat fluxes.

passing through the wall and the fluctuation of the heat flux will also be lower [24].

#### 4.3. Effect of thermophysical properties of composite on heat flux through the wall, heat flux time lag and decrement factor

The two parameters allow quantification of the thermal inertia of a building, the heat flux time lag  $\phi$ , which expresses the capacity of a construction element to store and release energy during the daily cycle, and the decrement factor  $f_d$ , are deduced from Fig. 15 which shows the temporal variations of the heat flux of the exterior surface and the variations of the heat flux of the interior surface of the studied walls. Fig. 16 shows the effects of adding date palm fibers to the studied earthen adobes on the two previous factors.

According to Fig. 16.a, the heat flux time lag is higher for the walls constructed by adobes made of earth reinforced with palms fibers in comparison with the one constructed by earth without fibers. It reaches the highest value of about 11.98 h for the case of walls constructed by earth mixed with pinnate leaf fibers; however, the values 11.21 h and 11.79 h were reached by the case of cluster and trunk fibers, respectively. These results can be explained by the effect of the two quantities thermal conductivity  $\lambda$  and volumetric thermal capacity  $\rho.c$  on the heat flux time lag.  $\phi$  increases with the decrease of  $\lambda$  and with the increase of  $\rho.c$  [24]. Indeed, even though the thermal conductivity of wall constructed of earth reinforced with trunk fibers ( $\lambda_{\text{trunk}} = 0.304 \text{ W}/(\text{m}^2 \cdot \text{K})$ ) is lower than that of case of reinforcement with cluster fibers ( $\lambda_{\text{cluster}} = 0.355 \text{ W}/(\text{m}^2 \cdot \text{K})$ ), the heat flux time lag in the first case was higher than that in the second case. This due to the effect of the volumetric thermal capacity which is important in the walls containing cluster fibers (( $\rho.c$ )<sub>cluster</sub> = 1263 KJ/(m<sup>3</sup> · K)) in comparison with that for the case of walls containing trunk fibers (( $\rho.c$ )<sub>trunk</sub> = 1010 KJ/(m<sup>3</sup> · K)). It is important to note that the higher values of the time lag of the heat flow ensure that the interior surface temperature of the wall reaches its maximum values during the night hours in summer. As the air temperature in the room reaches its minimum values around these night hours, there is a significant heat transfer from the wall surface to the indoor air and, consequently a lower consumption of electrical energy during the peak hours for cooling [24]. According to Fig. 16.b, the decrement factor  $f_d$  is higher for the walls

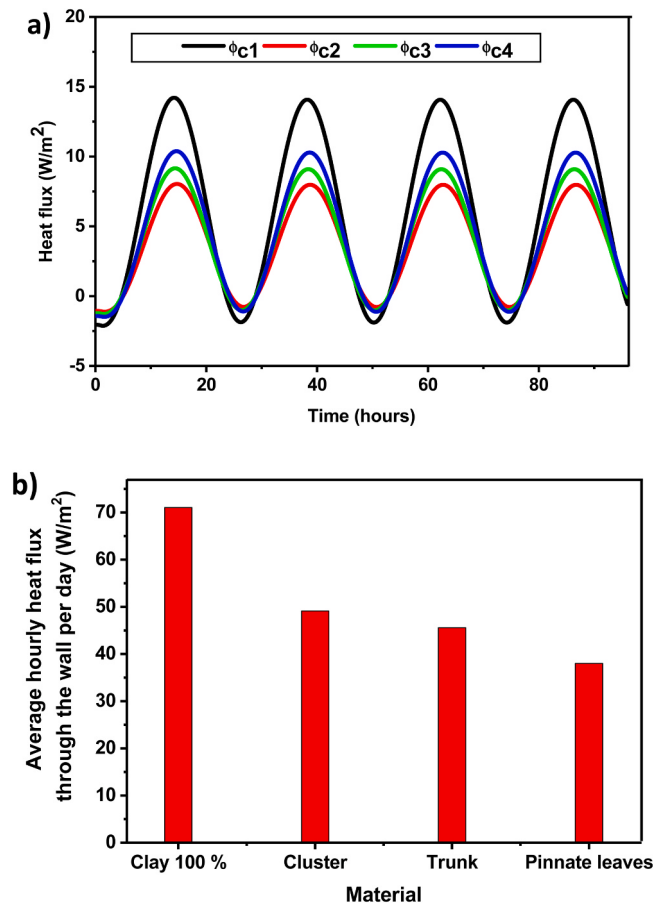


**Fig. 14.** Effects of various palm fibers used on: (a) the heat flux through the wall and (b) the average hourly heat flow through the wall per day  $\varphi_{cm}$ ,  $\varphi_{c1}$  heat flow through the wall without fibers,  $\varphi_{c2}$  heat flow through the wall containing pinnate leaf fibers,  $\varphi_{c3}$  heat flow through the wall containing trunk fibers and  $\varphi_{c4}$  heat flow through the wall containing cluster fibers.

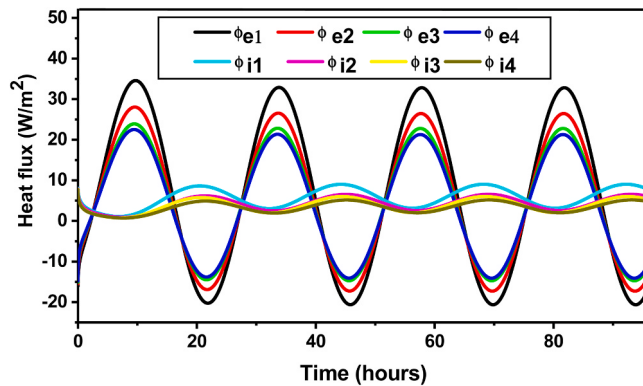


**Fig. 15.** Effects of various palm fibers used on the exterior surface heat flux and on the interior surface heat flux.  $\varphi_{e1}$  and  $\varphi_{i1}$  heat flux of the exterior and exterior surface of the wall without fibers,  $\varphi_{e2}$  and  $\varphi_{i2}$  heat flux of the exterior and exterior surface of the wall containing cluster fibers,  $\varphi_{e3}$  and  $\varphi_{i3}$  heat flux of the exterior and exterior surface of the wall containing trunk fibers,  $\varphi_{e4}$  and  $\varphi_{i4}$  heat flux of the exterior and exterior surface of the wall containing pinnate leaf fibers.

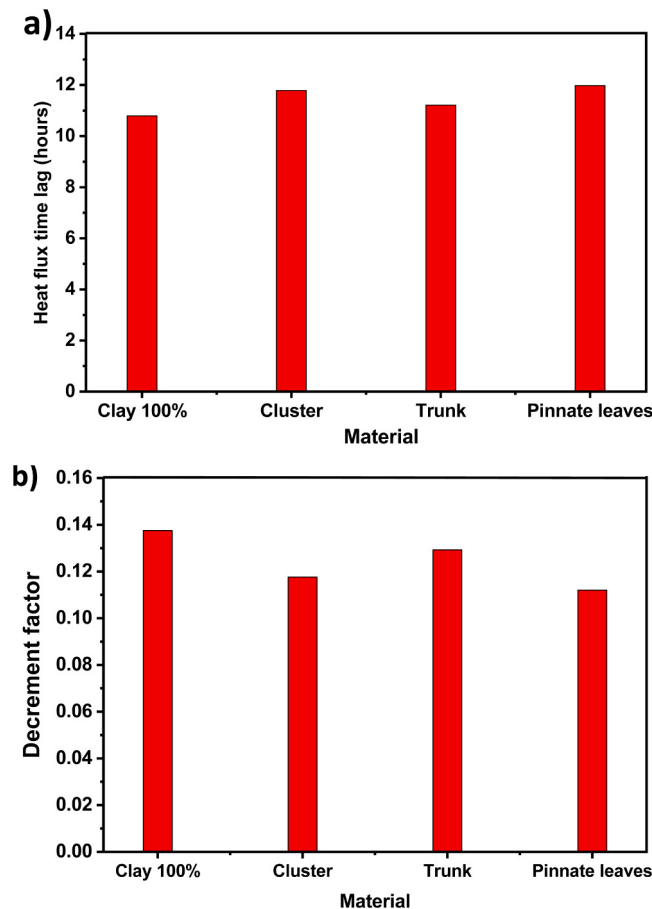


**Fig. 16.** Effects of various palm fibers used on: (a) the heat flux time lag and (b) the heat flux decrement factor.

constructed with earth without fibers about 0.14 compared to the one constructed with earth reinforced with palm fibers. In addition,  $f_d$  is lower for the case of pinnate leaf fibers about 0.11 followed by the case of cluster fibers and then the case of trunk fibers.

## 5. Conclusions

This work focused initially on an experimental study of the thermophysical properties of adobes based on raw earth reinforced with different date palm fibers: Pinnate leaves, Palm fiber mesh, Palm trunk, Petiole and Palm cluster, obtained from palms of the Drâa-Tafilalet region (Morocco). These fibers were added to five earth matrixes to obtain weight percentages from 0% to 6%. In a second step, a numerical simulation was carried out to evaluate the thermal performance of the walls built with these adobes. It is then a continuation of the work done on adobes containing a mixture of palm fibers. Our contribution is a comparative experimental and numerical study of the effects of the thermal properties of each fiber of the five parts of date palm wastes on the thermal performance of adobes and walls containing these fibers. The experimental study revealed on the one hand that the density of the samples containing 3% and 6% date palm fiber decreases on average by about 22% and 25% respectively. On the other hand, the thermal properties of the samples varied depending on the nature of the palm waste fibers and the fiber content. It was found that the thermal insulation improves by about 30% for a 6% mass fraction of petiole, palm fiber mesh and cluster fibers and by about 40% and 48% for a 6% mass fraction of trunk fibers and of pinnate leaf fibers respectively. In addition, the thermal damping is significantly improved for the samples containing the fibers of penna leaves, as its thermal diffusivity was reduced by about 26% and its thermal effusivity is decreased by up to 40%. The results of the numerical simulation show first of all a significant reduction of the hourly average heat flux per day passing through the walls constructed with adobes made of earth mixed with date palm fibers. This reduction is maximal for the walls contained the pinnate leaf fibers of about 46%. In a second time, the two parameters, the heat flux time lag and the heat

flux decrement factor, are determined to evaluate the thermal performance of the studied walls. It can be seen that the first parameter increased from 10.78 h to 11.98 h and the second decreased from 0.14 to 0.11 for the walls built with adobes made of raw earth mixed with 6% of the pinnate leaf fibers. As a result, a significant improvement in the thermal insulation and performance of earthen adobe and walls containing pinnate leaf fibers with a content of 6% has been observed.

## Declaration of Competing Interest

The authors declare that they have no known competing financial interests or personal relationships that could have appeared to influence the work reported in this paper.

## References

- [1] F. Aymerich, L. Fenu, P. Meloni, Effect of reinforcing wool fibres on fracture and energy absorption properties of an earthen material, *Construct. Build. Mater.* 27 (2012) 66–72, <https://doi.org/10.1016/j.conbuildmat.2011.08.008>.
- [2] U. Röhlen, C. Ziegert, A. Mochel, *Construire en terre crue: construction, rénovation, finitions*, Éd. Le Moniteur, Paris, 2013.
- [3] M. Lawrence, Reducing the environmental impact of construction by using renewable materials, *J. Renew. Mater.* 3 (2015) 163–174, <https://doi.org/10.7569/JRM.2015.634105>.
- [4] D. Gallipoli, G.W. Bruno, C. Perlot, J. Mendes, A geotechnical perspective of raw earth building, *Acta Geotech.* 12 (2017) 463–478.
- [5] S. Yang, S. Wia Jong, K. Hwayoung, L. Sumin Kima, Biochar-red clay composites for energy efficiency as eco-friendly building materials: thermal and mechanical performance, *J. Hazard. Mater.* 373 (2019) 844–855, <https://doi.org/10.1016/j.jhazmat.2019.03.079>.
- [6] M. Charai, S. Haitham, M. Ahmed, K. Mustapha, K. Elhammoutic, H. Nasric, Thermal performance and characterization of a sawdust-clay composite material, *Procedia Manuf.* 46 (2020) 690–697, <https://doi.org/10.1016/j.promfg.2020.03.098>.
- [7] R. Fernea, D.L. Manea, D.R. Tămasă-Gavrea, I.C. Roșca, Hemp-clay building materials – an investigation on acoustic, thermal and mechanical properties, *Procedia Manuf.* 32 (2019) 216–223, <https://doi.org/10.1016/j.promfg.2019.02.205>.
- [8] H. Binici, O. Aksogan, M. Nuri Bodur, E. Akca, S. Kapur, Thermal isolation and mechanical properties of fibre reinforced mud bricks as wall materials, *Construct. Build. Mater.* 21 (2007) 901–906, <https://doi.org/10.1016/j.conbuildmat.2005.11.004>.
- [9] K. ELAzhary, Y. Chihab, M. Mansour, N. Laaroussi, M. Garoum, Energy efficiency and thermal properties of the composite material clay-straw, *Energy Procedia* 141 (2017) 160–164, <https://doi.org/10.1016/j.egypro.2017.11.030>.
- [10] G. Desogus, S. Di Benedetto, R. Ricciu, The use of adaptive thermal comfort models to evaluate the summer performance of a Mediterranean earth building, *Energy Build.* 104 (2015) 350–359, <https://doi.org/10.1016/j.enbuild.2015.07.020>.
- [11] F. Hadji, N. Ihaddadene, R. Ihaddadene, A. Betga, A. Charick, P.O. Logerais, Thermal conductivity of two kinds of earthen building materials formerly used in Algeria, *J. Build. Eng.* 32 (2020), 101823, <https://doi.org/10.1016/j.jobe.2020.101823>.
- [12] M. Charaia, H. Sghouria, A. Mezrhaba, M. Karkrib, K. Elhammoutic, H. Nasri, Thermal performance and characterization of a sawdust-clay composite material, *Procedia Manuf.* 46 (2020) 690–697, <https://doi.org/10.1016/j.promfg.2020.03.098>.
- [13] K. Rashid, E.U. Haq, M.S. Kamran, N. Munir, A. Shahid, I. Hanif, Experimental and finite element analysis on thermal conductivity of burnt clay bricks reinforced with fibers, *Construct. Build. Mater.* 221 (2019) 190–199, <https://doi.org/10.1016/j.conbuildmat.2019.06.055>.
- [14] S. Ajouguim, S. Talibi, C. Djelal-Dantec, H. Hajjou, M. Waqif, M. Stefanidou, L. Saadi, Effect of Alfa fibers on the mechanical and thermal properties of compacted earth bricks, *Construct. Build. Mater.* 239 (2020), <https://doi.org/10.1016/j.conbuildmat.2019.117669>.
- [15] E. Olacia, A.L. Pisello, V. Chiodo, S. Maisano, A. Frazzica, L.F. Cabeza, Sustainable adobe bricks with seagrass fibres. Mechanical and thermal properties characterization, *Construct. Build. Mater.* 239 (2020), 117669.
- [16] P. Muñoz, V. Letelier, L. Muñoz, M.A. Bustamante, Adobe bricks reinforced with paper & pulp wastes improving thermal and mechanical properties, *Construct. Build. Mater.* 254 (2020), 119314, <https://doi.org/10.1016/j.conbuildmat.2020.119314>.
- [17] S. Liuzzi, C. Rubino, F. Martellotta, Properties of clay plasters with olive fibers, *Woodhead Publ. Ser. Civil Struct. Eng.* (2020) 171–186, <https://doi.org/10.1016/B978-0-12-819481-2.00009-X>.
- [18] A. Laborel-Préneron, C. Magniont, J.-E. Aubert, Hygrothermal properties of unfired earth bricks: effect of barley straw, hemp shiv and corn cob addition, *Energy Build.* 178 (2018) 265–278, <https://doi.org/10.1016/j.enbuild.2018.08.021>.
- [19] S. Maazouz Drâa-tafilalet: une région avec un fort potentiel agricole édition 2016.<https://www.agrimaroc.ma/draa-tafilalet-une-region-avec-un-fort-potentiel-agricole/>.
- [20] MAP DE DRÂA-TAFILALET RÉGION <http://mapecology.ma/slider/region-de-draa-tafilalet-413-mmdh-dinvestissements-filiere-palmier-dattier-entre-2010-2019/>.
- [21] A. Mellaikhafi, A. Tilioua, H. Souli, M. Garoum, M.A. Alaoui Hamdi, Characterization of different earthen construction materials in oasis of south-eastern Morocco (Errachidia Province), *Case Stud. Construct. Mater.* 14 (2021), e00496, <https://doi.org/10.1016/j.cscm.2021.e00496>.
- [22] D. Khoudja, B. Taallah, O. Izemmouren, S. Aggoun, O. Herihiri, A. Guettala, Mechanical and thermophysical properties of raw earth bricks incorporating date palm waste, *Construct. Build. Mater.* 270 (2021), 121824, <https://doi.org/10.1016/j.conbuildmat.2020.121824>.
- [23] H. Asan, Y.S. Sancaktar, Effects of Wall's thermophysical properties on time lag and decrement factor, *Energy Build.* 28 (1998) 159–166, [https://doi.org/10.1016/S0378-7788\(98\)00007-3](https://doi.org/10.1016/S0378-7788(98)00007-3).
- [24] X. Jin, X. Zhang, Y. Cao, G. Wang, Thermal performance evaluation of the wall using heat flux time lag and decrement factor, *Energy Build.* 47 (2012) 369–374, <https://doi.org/10.1016/j.enbuild.2011.12.010>.
- [25] C.R. Ruivo, P.M. Ferreira, D.C. Vaz, On the error of calculation of heat gains through walls by methods using constant decrement factor and time lag values, *Energy Build.* 60 (2013) 252–261, <https://doi.org/10.1016/j.enbuild.2013.02.001>.
- [26] Moussa Ouedraogo, Kalifata Dao, Younoussa Millogo, Jean-Emmanuel Aubert, Adamah Messan, Mohamed Seynou, Lamine Zerbo, Moussa Gomina, Physical, thermal and mechanical properties of adobes stabilized with fonio (*Digitaria exilis*) straw, *J. Build. Eng.* 23 (2019) 250–258, <https://doi.org/10.1016/j.jobe.2019.02.005>.
- [27] Y. Millogo, J.-E. Aubert, A.D. Sére, A. Fabbri, J.-C. Morel, Earth Blocks Stabilized by Cow-dung (Springer Verlag), in: *Materials and Structures*, 2016, pp. 4583–4594 (Springer Verlag), (<https://link.springer.com/article/10.1617/s11527-016-0808-6>).
- [28] NF P94-056, *Sols: reconnaissance et essais - Analyse granulométrique - Méthode par tamisage à sec après lavage*, 1996.
- [29] NF P94-057, *Sols: reconnaissance et essais - Analyse granulométrique des sols - Méthode par sédimentation*, 1992.
- [30] B. Hay, J.R. Filtz, J.C. Batsale, Mesure de la diffusivité thermique par la méthode flash, *R 2 995, Techniques de l'ingénieur*, 33 (2004). R 2 995.

- [31] le règlement parasismique pour les constructions en terre et instituant le Comité national des constructions en terre, Maroc, Décret n° 2-12-666 du 17 rejab 1434, 28 mai 2013.
- [32] Le Palmier Dattier base de la mise en valeur des oasis au Maroc, Techniques phoenicole et Crédit d'oasis. Institut National de la Recherche Agronomique Maroc.
- [33] R.A. Nasser, M.Z.M. Salem, S. Hiziroglu, H.A. Al-Mefarrej, A.S. Mohareb, M. Alam, I.M. Aref, Chemical analysis of different parts of date palm (*Phoenix dactylifera L.*) using ultimate, proximate and thermo-gravimetric techniques for energy production, Energies 9 (5) (2016) 374. (<https://www.mdpi.com/1996-1073/9/5/374>).
- [34] P. Brzyski, P. Kosiski, A. Skoratko, W. Motacki, Thermal properties of cellulose fiber as insulation material in a loose state, AIP Conference Proceedings 2133 (2019), 020006, <https://doi.org/10.1063/1.5120136>.
- [35] M. Boumhaout, L. Boukhattem, H. Hamdi, B. Benhamou, F. Ait Nouh, Thermomechanical characterization of a bio-composite building material: Mortar reinforced with date palm fibers mesh, Construct. Build. Mater. 135 (2017) 241–250, <https://doi.org/10.1016/j.conbuildmat.2016.12.217>.